

**Integrated process development for microalgae assisted
coal mine effluent treatment and microalgae-low rank
coal blended fuel production**



**Thesis submitted in partial fulfilment
for the award of degree
Doctor of philosophy**

By

SHWETA RAWAT

**SCHOOL OF BIOCHEMICAL ENGINEERING
INDIAN INSTITUTE OF TECHNOLOGY
(BANARAS HINDU UNIVERSITY)
VARANASI – 221 005**


20011507

2024

CERTIFICATE

It is certified that the work contained in the thesis titled “**Integrated process development for microalgae assisted coal mine effluent treatment and microalgae-low rank coal blended fuel production**” by **Shweta Rawat** has been carried out under my supervision and that this work has not been submitted elsewhere for a degree.

It is further certified that the student has fulfilled all the requirements of Comprehensive, Candidacy and SOTA.


Dr. Sanjay Kumar
(Supervisor)
School of Biochemical Engineering
Indian Institute of Technology
(Banaras Hindi University)
Varanasi-221005

डॉ. संजय कुमार
Dr. Sanjay Kumar
सह आचार्य
Associate Professor
School of Biochemical Engineering
Indian Institute of Technology
(Banaras Hindi University) Varanasi
Varanasi-221005, उत्तर प्रदेश, भारत
Varanasi 221005, Uttar Pradesh, India

DECLARATION BY THE CANDIDATE

I, **Shweta Rawat**, certify that the work embodied in this thesis is my own bona fide work and carried out by me under the supervision of **Dr. Sanjay Kumar** from **January 2021** to **August 2024**, at the **School of Biochemical Engineering, Indian Institute of Technology, Varanasi**. The matter embodied in this thesis has not been submitted for the award of any other degree/diploma. I declare that I have faithfully acknowledged and given credits to the research workers wherever their works have been cited in my work in this thesis. I further declare that I have not willfully copied any other's work, paragraphs, text, data, results, *etc.*, reported in journals, books, magazines, reports dissertations, theses, *etc.*, or available at websites and have not included them in this thesis and have not cited as my own work.

Date: 7/8/2024

Place: Varanasi

Shweta Rawat
Shweta Rawat

CERTIFICATE BY THE SUPERVISOR

It is certified that the above statement made by the student is correct to the best of my knowledge.

Sanjay Kumar
Dr. Sanjay Kumar
(Supervisor)
School of Biochemical Engineering
Indian Institute of Technology
(Banaras Hindi University),
Varanasi-221005

डॉ. संजय कुमार
Dr. Sanjay Kumar
सह आचार्य
Associate Professor
जैव रासायनिक अभियांत्रिकी स्कूल
School of Biochemical Engineering
(संजय) वाराणसी
Indian Institute of Technology (IIT) Varanasi
वाराणसी-221005, उत्तर प्रदेश, भारत
Varanasi-221005, Uttar Pradesh, India

Fernandez
Vilchunse Day
Coordinator
जैव रासायनिक अभियांत्रिकी स्कूल
School of Biochemical Engg
भारतीय प्रौद्योगिकी संस्थान
Indian Institute of Technology
(का०हि०वि०वि०) वाराणसी-221005
(IIT) Varanasi-221005

Signature of Head of Department/Coordinator of School

COPYRIGHT TRANSFER CERTIFICATE

Title of the Thesis: **Integrated process development for microalgae assisted coal mine effluent treatment and microalgae-low rank coal blended fuel production.**

Name of the Student: **Shweta Rawat**

Copyright Transfer

The undersigned hereby assigns to the Institute of Technology (Banaras Hindu University) Varanasi all rights under copyright that may exist in and for the above thesis submitted for the award of the Ph.D. degree.

Date: **7/8/2024**

Place: Varanasi

Shweta Rawat
Shweta Rawat

Note: However, the author may reproduce or authorize others to reproduce material extracted verbatim from the thesis or derivative of the thesis for author's personal use provided that the source and the Institute's copyright notice are indicated.

**Dedicated to my mentors,
parents, family and extended
family**

ACKNOWLEDGEMENT

Through this page, I offer my salutation to **Mahamana Pt. Madan Mohan Malviya Ji**, the creator of this pious seat of learning.

It is indeed my proud privilege to express my deep sense of gratitude, respect, indebtedness and sincere regards to **Dr. Sanjay Kumar, my Supervisor, School of Biochemical Engineering, Indian Institute of Technology (Banaras Hindu University), Varanasi** for his excellent supervision, skilled and valuable guidance, stimulating discussion, unfailing support, immense help and constant encouragement over entire period of my association with him. I am grateful to him for his sincere concern both for academics and personal welfare and care throughout the research period that he has extended to me for the successful completion of my research work. I am proud to have a teacher like him who is always motivative and supportive, even in most adverse situations. In fact, he has been a source of inspiration for me to have an optimistic approach in life and do my best.

I thank **Prof. Vikash Kumar Dubey, HOD School of Biochemical Engineering, IIT(BHU) Varanasi** for providing all support and lab facilities to conduct experiments. I am also thankful to **Prof. Ram Sharan Singh, QIP coordinator, IIT(BHU) Varanasi** to guide me related to QIP related task.

I would like to express my deepest gratitude to my **RPEC committee members, Dr. Pranjal Chandra, School of Biochemical Engineering, IIT(BHU)** and **Dr. Ankur Verma, Department of Chemical Engineering & Technology, IIT (BHU)** for their fruitful suggestions into my work and their efforts to increase the overall quality of my work outputs.

I wish to express my sincere thanks to **Dr. Jyoti Prasad Chakraborty, Department of Chemical Engineering & Technology, IIT (BHU)** for helping in my experiments. I express

my heartfelt thanks to **Dr. Vigya Kesari** to give me valuable suggestions throughout my research period.

I am again thankful to **Dr. Pranjal Chandra, DPGC Convener, School of Biochemical Engineering, IIT (BHU)** for his constant support and guidance.

I thank all the respected **faculty members of School of Biochemical Engineering, IIT(BHU), Dr. Abha Mishra, Dr. Abhishek S. Dhoble, Dr. Aditya K. Padhi, Dr. Pranjal Chandra, Dr. Prodyut Dhar, Dr. Rajendra Meena, Dr. Sharon Mano Pappu J, Dr. Sumit Singh and Dr. Vishal Mishra** who have helped me a lot in overcoming the bottlenecks, I encountered during my studies with their valuable advices. I would also like to acknowledge **technical and non-technical staff** for their support throughout my Ph.D.

I have been surrounded by some outstanding seniors, batchmates, and juniors throughout my PhD journey. I express my heartfelt thanks to **Biofuels Research Lab Team, Mr. Indrajeet Yadav, Mr. Akhil Rautela, Mr. Agendra Gangwar, Ms. Rishika Chatterjee and Mrs. Akanksha Singh** who played an instrumental role during my PhD journey.

I would like to express my deepest gratitude to **my parents, Mr. Pratap Singh Rawat and Mrs. Malti Rawat** for their blessings and consistent support throughout my PhD journey. I am in debt to my family members **my husband, Mr. Chandan Singh Bhakuni** and son **Bhavyansh Bhakuni** for their constant motivation and emotional support. I am also thankful to **my sister, Mrs. Swati Tripathi** for her kindness and support.

I take this occasion to acknowledge the **All India Council for Technical Education (AICTE)** to provide me opportunity to pursue PhD under **Quality Improvement Programme (QIP)** to upgrade the expertise and capabilities as a faculty member. I wish to express thanks to **my organization, Bipin Tripathi Kumaon Institute of Technology, Dwarahat** to provide me three years study leave to pursue PhD. Again, I wish to express a word of thanks to all those

hands that helped me in some way or the other in pursuing my research work and for the completion of thesis. Finally, I bow my head humbly before the **Almighty God** without whose consent and blessings, this work would have been impossible.

Date:

Place: **IIT (BHU), Varanasi**

(SHWETA RAWAT)

TABLE OF CONTENT

Chapter – 1	Introduction to integrated strategies for coal mine effluent treatment and biofuel production	1
	Abstract	2
1.1	Introduction	3
1.2	Conventional strategies for coal mine effluent treatment	5
1.3	Environmental impacts of conventional treatment	6
1.4	Renewable energy technologies integrated with coal mine effluent treatment	7
1.5	Approach	7
1.6	Objectives	10
1.7	Thesis outline	12
Chapter – 2	Review of literature on coal mine effluent treatment, resource utilization and fuel production using microalgae platform	14
	Abstract	15
2.1	Background	16
2.2	Methods to treat coal mine effluent	18
2.2.1	Biological methods to treat coal mine effluent	18
2.2.2	Microalgae mediated coal mine effluent treatment	20
2.2.2.1	Biodesalination process using microalgae platform	22
2.2.2.2	Role of microalgae in heavy metal removal	24
2.2.2.3	Mechanism of biodesalination and heavy metal removal	27
2.2.3	Biofuel production from harvested microalgae biomass	30
2.2.3.1	Transesterification for biodiesel production	31
2.2.3.2	Mechanical conversion for solid briquette production	36
2.2.3.3	Thermochemical conversion for bio-oil, bio-char and bio-gas production	40
2.4	Identified research gaps	45
Chapter – 3	Screening and selection of candidate microalgae based on coal mine effluent bioremediation and thermal properties assessment	47
	Abstract	48
3.1	Background	49
3.2	Materials and methods	51
3.2.1	Microalgae and culture condition	51
3.2.2	Coal mine water collection, characterization and microalgae habitation	51
3.2.3	Microalgae harvesting and pretreatment for thermal properties estimation	52
3.2.4	Screening of fresh and marine algal isolates based on cell growth and nutrient removal	53
3.2.4.1	Microalgae screening based on growth kinetics analysis	54
3.2.4.2	Microalgae screening based on salinity and chemical oxygen demand (COD) removal	55
3.2.4.3	Elemental and biochemical analysis of biomass	55
3.2.5	Microalgae screening based on thermal characteristic analysis	56
3.2.5.1	Fuel characteristic analysis of microalgae samples	56
3.2.5.2	Thermogravimetric and Fourier transform infrared analysis	57
3.2.5.3	Kinetic analysis of microalgae biomass pyrolysis	58
3.2.5.4	Thermodynamic properties estimation of different microalgae biomass	61
3.2.5.5	Deep neural network data processing and model designing	61
3.3	Results and discussion	63
3.3.1	Physical and chemical characterization of coal mine effluent	63
3.3.2	Growth and screening of potential microalgae in nutrient supplemented coal mine effluent	64
3.3.3	Fuel characteristic analysis of fresh and marine microalgal biomass	67
3.3.3.1	One-way ANOVA and Spearman’s rank correlation for fuel characteristic variables	70
3.3.4	Fourier transform infrared spectroscopy analysis	72

3.3.5	Thermal decomposition behavior of microalgae	73
3.3.5.1	Effect of heating rate upon microalgae thermal decomposition	74
3.3.6	Kinetic analysis of freshwater and marine microalgae species	77
3.3.6.1	Coats Redfern method	77
3.3.6.2	Distributed activation energy model approach	81
3.3.6.3	Thermodynamic properties analysis	85
3.3.7	Thermal behavior prediction by Deep neural network (DNN) simulation	87
3.3.7.1	Optimization of the Conv 1D-LSTM model	87
3.4	Conclusion	91
Chapter – 4	Coal mine effluent treatment by semi-continuous cultivation of candidate microalgae in reactor scale	92
	Abstract	93
4.1	Background	94
4.2	Materials and methods	95
4.2.1	Indoor batch and semi-continuous cultivation	95
4.2.2	Analytical methods	96
4.2.3	Lipid extraction and determination of fatty acid methyl esters composition	97
4.2.4	Statistical analysis	98
4.3	Results and discussions	98
4.3.1	Biomass and lipid productivities of <i>C. pyrenoidosa</i> sp. in semi-continuous cultivation	99
4.3.2	Nutrient removal performance at different hydraulic retention time in semi-continuous cultivation	102
4.3.3	Fatty acid methyl ester analysis of candidate <i>C. pyrenoidosa</i> sp. cultivated in NSCME	105
4.3.4	FTIR analysis of microalgal biomass, lipid extracted microalgal biomass and oil	107
4.3.5	Biodesalination and heavy metal remediation from NSCME using <i>C. pyrenoidosa</i> sp.	109
4.3.6	Large scale implementation strategy of developed water treatment process at coal mine site	111
4.4	Conclusion	114
Chapter – 5	Co-investigation of mechanical performance and thermal behavior of de-oiled microalgae blended coal composites	115
	Abstract	116
5.1	Background	117
5.2	Materials and methods	119
5.2.1	Sampling, processing and basic fuel characterization of raw sample	119
5.2.2	Microalgae-blended coal composite preparation and characterization	120
5.2.3	Mechanical, thermal and Fourier transform infrared analysis of composites	121
5.2.4	Statistical modeling and analysis	122
5.2.5	Uncertainty analysis	123
5.2.6	Artificial neural network simulation	123
5.3	Results and discussions	123
5.3.1	Impact of pelleting material on fuel characteristics of composites	123
5.3.2	Optimization of process variables to maximize the mechanical performance of microalgae blended coal pellets	125
5.3.3	Pelletizing process variables optimization to maximize the individual response	128
5.3.4	Multi-response optimization analysis	133
5.3.5	Model validation	135
5.3.6	Fourier transform infrared analysis	136
5.3.7	Thermogravimetric analysis	140
5.3.8	Artificial neural network simulation	145
5.4	Conclusion	148

Chapter – 6		150
	Abstract	151
6.1	Background	152
6.2	Materials and methods	154
6.2.1	Feedstock processing and characterization of blended materials	154
6.2.2	Thermogravimetric and kinetic analysis	155
6.2.3	TG-FTIR experiments	156
6.2.4	Statistical analysis of coal and de-oiled microalgae blends thermal characteristic variables	157
6.2.5	Response surface and statistical modeling	157
6.2.6	Artificial neural network aided multi-objective genetic algorithm model development	158
6.3	Results and discussion	161
6.3.1	Fuel analysis	161
6.3.2	Thermogravimetric analysis	162
6.3.3	Kinetic Analysis of coal and de-oiled microalgae blended material	164
6.3.4	Syngas emission analysis during co-pyrolysis of coal and de-oiled microalgae blended material	169
6.3.5	Statistical optimization of process variables to enhance hydrogen carrying ratio and analysis	171
6.3.6	Integrated ANN-MOGA model development for hydrogen enhancement	176
6.3.7	Model validation and comparative assessment of RSM and ANN-MOGA	178
6.4	Conclusion	182
Chapter – 7	Co-pyrolysis of low-rank coal and de-oiled microalgae biomass for bio-oil production using synthesized catalyst	184
	Abstract	185
7.1	Background	186
7.2	Materials and methods	188
7.2.1	Materials	188
7.2.2	Catalyst preparation and characterization	189
7.2.3	Noncatalytic and catalytic pyrolysis of coal and/or de-oiled microalgae	191
7.2.4	Pyrolysis end-products distribution and energy calculations	192
7.2.5	Characteristics of noncatalytic and catalytic pyrolysis bio-oil	193
7.3	Results and discussion	194
7.3.1	Characterization of synthesized Cu-Cr-ZSM-5 catalyst	194
7.3.1.1	X-ray diffraction	194
7.3.1.2	Microstructure characterization	195
7.3.1.3	Fourier Transform Infrared analysis	197
7.3.1.4	Brunauer-Emmett-Teller (BET) surface area analysis	199
7.3.2	Thermal characteristics of catalyst and pyrolysis feedstocks	200
7.3.3	Product yield distribution from non-catalytic and catalytic pyrolysis	201
7.3.4	Bio-oil characteristics from non-catalytic and catalytic pyrolysis	204
7.3.4.1	Fourier transform infrared spectroscopy of bio-oil	204
7.3.4.2	GS-MS of catalytic and non-catalytic pyrolysis bio-oil	206
7.3.4.3	Physicochemical characteristics of bio-oil from non-catalytic and catalytic pyrolysis	213
7.3.5	Proposed mechanism for catalytic upgradation of bio-oil applying synthesized Cu-Cr-ZSM-5 catalyst	215
7.4	Conclusion	219
Chapter – 8	Conclusion and future perspectives	220
References		225
Appendix		246

LIST OF FIGURES

Fig. 1.1	(a) Active coal mines existing in different countries (b) adverse environmental impact of coal fines and water interaction.	4
Fig. 1.2	Negative environmental impact of coal mine water drainage.	4
Fig. 2.1	Commercial applications of microalgae as a potential reservoir of bioenergy.	20
Fig. 2.2	Schematic representation of microalgae culture systems to treat coal mine water and biofuel or other value-added product formation.	21
Fig. 2.3	Conceptual representation of coal mine effluent biodesalination using microalgae platform.	22
Fig. 2.4	Proposed biodesalination mechanism and type of interactions involved in bioadsorption and bioaccumulation of Na^+ and Cl^- in microalgae cell.	29
Fig. 2.5	Mechanism involved in heavy metal removal from coal mine effluent by using microalgae.	30
Fig. 2.6	Process strategies to formulate different coal – biomass composites.	37
Fig. 2.7	(a) Process design for de-oiled microalgae blended coal briquette production (b) schematic diagram of briquetting machine.	38
Fig. 2.8	Process design for carbonized de-oiled microalgae biomass or charcoal briquettes production.	38
Fig. 3.1	Selection flow chart of candidate microalgae for coal mine effluent treatment and bio-fuel production.	53
Fig. 3.2	Growth profiles of fresh and marine microalgae strains – <i>Chlorella pyrenoidosa</i> (CPY), <i>Chlorella minutissima</i> (CM), <i>Chlorella protothecoides</i> (CPR), <i>Chlorella vulgaris</i> (CV), <i>Dunaliella sp.</i> (DU) in (a) coal mine effluent (CME) (b) nutrient supplemented coal mine effluent (NSCME).	65
Fig. 3.3	Nutrient removal efficiency (%) of fresh and marine microalgae strains in (a) coal mine effluent (CME) (b) nutrient supplemented coal mine effluent (NSCME).	66
Fig. 3.4	FTIR spectrum of de-oiled microalgae.	72
Fig. 3.5	Thermal analysis (a) TG curves (b) DTG curves of pyrolysis of de-oiled microalgae at the heating rate of 10 °C/min.	73
Fig. 3.6	TG curves for the pyrolysis of de-oiled microalgae at the heating rate of 10, 20 and 30 °C/min (a) <i>Chlorella pyrenoidosa</i> (CPY) (b) <i>Chlorella minutissima</i> (CM) (c) <i>Chlorella protothecoides</i> (CPR) (d) <i>Chlorella vulgaris</i> (CV) (e) <i>Dunaliella sp.</i> (DU).	75
Fig. 3.7	DTG curves for the pyrolysis of de-oiled microalgae at the heating rate of 10, 20 and 30 °C/min (a) <i>Chlorella pyrenoidosa</i> (CPY) (b) <i>Chlorella minutissima</i> (CM) (c) <i>Chlorella protothecoides</i> (CPR) (d) <i>Chlorella vulgaris</i> (CV) (e) <i>Dunaliella sp.</i> (DU).	76
Fig. 3.8	Best fitted Coats Redfern kinetic models based on solid state diffusion for main pyrolysis stage (230–370 °C) of de-oiled microalgae. (a) <i>Chlorella pyrenoidosa</i> (CPY), (b) <i>Chlorella minutissima</i> (CM), (c) <i>Chlorella protothecoides</i> (CPR), (d) <i>Chlorella vulgaris</i> (CV), (e) <i>Dunaliella sp.</i> (DU) (f) Regression coefficient (R^2) and activation energy (E_a) estimation.	80

Fig. 3.9	Acceptability order of Coats Redfern kinetic models based on coefficient of determination (R^2) for different de-oiled microalgae species (a) <i>Chlorella pyrenoidosa</i> (CPY) (b) <i>Chlorella minutissima</i> (CM) (c) <i>Chlorella protothecoides</i> (CPR) (d) <i>Chlorella vulgaris</i> (CV) (e) <i>Dunaliella sp.</i> (DU).	81
Fig. 3.10	Distributed activation energy model (DAEM) of (a) <i>Chlorella pyrenoidosa</i> (CPY) (b) <i>Chlorella minutissima</i> (CM) (c) <i>Chlorella protothecoides</i> (CPR) (d) <i>Chlorella vulgaris</i> (CV) (e) <i>Dunaliella sp.</i> (DU) at a heating rate of 10, 20 and 30°C/min for mass conversion ratio ($\alpha = 0.1-0.9$).	83
Fig. 3.11	Thermodynamic properties estimation of de-oiled microalgae (a) Activation energy (E_a) (b) Enthalpy change (ΔH) (c) Gibbs free energy change (ΔG) (d) Entropy change (ΔS) for mass conversion ratio ($\alpha=0.1-0.9$).	84
Fig. 3.12	Deep neural network architecture to predict thermal behavior of de-oiled microalgae <i>Chlorella pyrenoidosa</i> .	88
Fig. 3.13	Comparative assessment of experimental and predicted pyrolysis of de-oiled microalgae <i>Chlorella pyrenoidosa</i> at a heating rate (°C/min) of (a) 10 (b) 20 (c) 30. Variation of training and validation loss with number of epochs at a heating rate (°C/min) of (d) 10 (e) 20 (f) 30.	90
Fig. 4.1	Schematic representation of the pilot scale indoor experimental set-up of bubble column reactor and open raceway pond for semi-continuous treatment of coal mine effluent.	98
Fig. 4.2	Biomass concentration (g L^{-1}) and lipid contents (%) of candidate microalgae <i>Chlorella pyrenoidosa</i> in nutrient supplemented coal mine effluent cultivated in semi-continuous mode (a,c,e) Bubble column reactor (BCR), (b,d,f) Open raceway pond (ORP).	100
Fig. 4.3	Biomass productivity ($\text{mg L}^{-1} \text{d}^{-1}$) of microalgae at different hydraulic retention time (HRT) during batch and semi-continuous cultivation mode in bubble column photobioreactor (BCR) and open raceway pond (ORP).	101
Fig. 4.4	Chemical oxygen demand (mg L^{-1}) and electric conductivity (mS cm^{-1}) variation of nutrient supplemented coal mine effluent during semi-continuous mode (a, c, e) Bubble column photobioreactor (BCR) (b, d, f) Open raceway pond (ORP).	103
Fig. 4.5	Nutrient removal (%) at different hydraulic retention time (HRT) during semi-continuous cultivation mode in bubble column photobioreactor (BCR) and open raceway pond (ORP).	104
Fig. 4.6	FTIR spectrum of (a) BG-11 grown microalgae (b) Nutrient supplemented coal mine effluent grown microalgae (c) De-oiled nutrient supplemented coal mine effluent grown microalgae (d) Extracted lipid from nutrient supplemented coal mine effluent grown microalgae (e) Fatty acid methyl ester from nutrient supplemented coal mine effluent grown microalgae.	108
Fig. 4.7	SEM micrograph and elemental mapping of salts and heavy metals assimilated in microalgae <i>C. pyrenoidosa</i> (a) harvested after end cycle of HRT 6 d through semi-continuous cultivation (b) microalgae at start of cycle ($t = 0$ d) (c) comparison of elemental mapping at end cycle of HRT 6 d and $t = 0$ d.	110

Fig. 4.8	Long term outdoor microalgae cultivation in coal mine site (a) flow diagram representing active microalgae-based wastewater treatment with possible water and land outcomes (b) potential environmental and social implications of microalgae production at coal mine site.	112
Fig. 5.1	Low-rank coal excavation from Amelia coal block.	119
Fig. 5.2	Schematic representation of microalgae blended coal composite (MBCC) production.	120
Fig. 5.3	Three-dimensional response surface plot of compressive strength (a-c) and drop strength (d-f) for microalgae blended coal composite (MBCC) production with varying molding pressure (MPa) vs average particle size (mm), molding pressure (MPa) vs binder ratio (%), average particle size (mm) vs binder ratio (%) respectively; the third variable was kept at central value.	132
Fig. 5.4	Individual optimization plot to maximize (a) compressive strength (b) drop strength for microalgae blended coal composite (MBCC) production.	133
Fig. 5.5	Multi-objective optimization plot to maximize compressive strength and drop strength for microalgae.	134
Fig. 5.6	Contour plot for cumulative maximization of responses with varying variables, (a) molding pressure (MPa) vs binder ratio (%) (b) average particle size (mm) vs binder ratio (%) (c) molding pressure (MPa) vs average particle size (mm); the third variable was kept at central value.	135
Fig. 5.7	FTIR spectra of microalgae, raw coal, individual optimized and multi-objective optimized microalgae blended coal composite (MBCC): MBCC1 (for compressive strength optimization), MBCC2 (for drop strength optimization), MBCC3 (for multi-objective optimization).	139
Fig. 5.8	TGA-DTG-DTA plot of (a) raw coal (b) microalgae (<i>C. pyrenoidosa</i>) (c) individual optimized MBCC1 (for compressive strength optimization) (d) individual optimized MBCC2 (for drop strength optimization) (e) multi-objective optimized MBCC3 (f) morphological appearance of raw coal, microalgae, and MBCCs.	142
Fig. 5.9	ANN Regression plots of training, validation and testing stages (a) coal (b) de-oiled microalgae (c) multi-objective optimized microalgae blended coal composite, respectively.	146
Fig. 5.10	Validation performance of Mean square error (MSE) for TGA data at a heating rate of 10 °C/min and 18 neuron numbers (a) coal (b) microalgae (<i>C. pyrenoidosa</i>) (c) multi-objective optimized microalgae blended coal composite.	147
Fig. 5.11	Error histogram for TGA data at a heating rate of 10 °C/min and 18 neuron numbers (a) coal (b) microalgae (<i>C. pyrenoidosa</i>) (c) multi-objective optimized microalgae blended coal composite.	148
Fig. 6.1	Schematic representations (a) experimental work flow associated with optimization model development and validation (b) feedforward artificial neural network (ANN) architecture consisting of two neurons input layer, ten neurons hidden layer and three neurons output layer integrated with multi-objective genetic algorithm (MOGA) model.	160
Fig. 6.2	Fuel analysis of coal and de-oiled microalgae blends (a) moisture content (MC), volatile matter (VM), fixed carbon (FC) and ash content (A) analysis (b) oxygen/carbon (O/C), hydrogen/carbon (H/C), fuel ratio (FR) and high heating value (HHV) analysis.	162

Fig. 6.3	(a) TG profile for coal and de-oiled microalgae blends (b) DTG profile for coal and de-oiled microalgae blends at heating rate (β) of 10 °C/min.	164
Fig. 6.4	Pyrolysis kinetic analysis over a range of mass conversion ratio ($\alpha = 0.1$ to 0.9) by Kissinger - Akahira - Sunose (KAS) method.	165
Fig. 6.5	Pyrolysis kinetic analysis over a range of mass conversion ratio ($\alpha = 0.1$ to 0.9) by Starink (STK) method.	166
Fig. 6.6	Activation energy (E_a) estimation for (a) coal and de-oiled microalgae blends (b) individual de-oiled microalgae over a range of mass conversion ratio ($\alpha=0.1$ to 0.9) by using Kissinger-Akahira-Sunose (KAS) method and Starink (STK) method.	168
Fig. 6.7	Syngas emission analysis by TG-FTIR at pyrolysis characteristic temperatures for coal and de-oiled microalgae blends (a) CL ALG 1-0 (b) CL ALG 3-1 (c) CL ALG 1-1 (d) CL ALG 1-3 (e) CL ALG 0-1.	170
Fig. 6.8	RSM-based CCD optimization (a) 3-D response surface plots (b) overlaid contour plot (c) multi-objective optimization plot to maximize Y_1 , Y_2 and Y_3 – hymethane carrying ratio at T_{p1} , T_{p2} and T_{p3} respectively.	175
Fig. 6.9	ANN-MOGA modeling to enhance hymethane carrying ratio (a) error histogram (b) pareto front for multi-objective optimization (c) mean square error vs epoch plot (d) performance through validation check plot (e) regression plots displaying training, validation and test models with regression coefficient values.	177
Fig. 6.10	Experimental validation of hymethane carrying ratio and syngas distribution at (a) CL ALG 1-1 (blending ratio: 50%) (b) statistical optimized (RSM) (c) ANN - MOGA optimized condition.	179
Fig. 6.11	TG-FTIR spectrum for gaseous product emission at different pyrolysis characteristic temperatures for (a) CL ALG 1-1 (blending ratio: 50%) (b) statistical optimized (RSM) (c) ANN-MOGA optimized condition.	181
Fig. 6.12	3-D infrared spectra for multi-objective optimization to maximize hymethane carrying ratio at (a) CL ALG 1-1 (blending ratio: 50%) (b) statistical optimized (RSM) (c) ANN-MOGA optimized condition.	182
Fig. 7.1	Schematic representation of one-pot synthesis strategy of Cu-Cr-ZSM-5 catalyst.	190
Fig. 7.2	Catalytic co-pyrolysis of coal and de-oiled microalgae blend in fixed bed reactor (a) schematic diagram of fixed bed reactor (b) co-pyrolysis set-up (c) experimental conditions of catalytic co-pyrolysis.	191
Fig. 7.3	Typical XRD pattern of synthesized Cu-Cr-ZSM-5 and parent ZSM-5 catalyst.	195
Fig. 7.4	(a) SEM micrograph of synthesized Cu-Cr-ZSM-5 catalyst (b) Elemental mapping of carbon, aluminum, silicon, oxygen, copper, and chromium with weight % distribution in synthesized Cu-Cr-ZSM-5 catalyst.	197
Fig. 7.5	TEM images of (a,b,c,d,f) synthesized Cu-Cr-ZSM-5 catalyst at different resolutions (e) SAED pattern of synthesized Cu-Cr-ZSM-5 catalyst.	198
Fig. 7.6	FTIR spectra of parent ZSM-5 catalyst and synthesized Cu-Cr-ZSM-5 catalyst at different pyrolysis stages.	199

Fig. 7.7	(a) BET surface area analysis (b) N ₂ adsorption-desorption isotherms (c) pore size distribution (d) textural characteristics of synthesized Cu-Cr-ZSM-5 catalyst.	200
Fig. 7.8	(a) TG profile (b) DTG profile for coal and de-oiled microalgae blend with different ratios of catalyst.	201
Fig. 7.9	Product yield distribution (%) of char, aqueous product, bio-oil and gas from non-catalytic and catalytic pyrolysis of coal (CL), microalgae (ALG) and coal-microalgae blend (CLALG) with the synthesized catalyst at different ratios (0.5:1, 1:1 and 2:1).	202
Fig. 7.10	FTIR spectra of bio-oil derived from non-catalytic and catalytic pyrolysis of coal (CL), microalgae (ALG) and coal-microalgae (CLALG) blend with synthesized Cu-Cr-ZSM-5 catalyst at ratio of 1:1.	205
Fig. 7.11	GC-MS spectrum of bio-oil from pyrolysis of coal (CL), microalgae (ALG) and coal-microalgae (CLALG) blend (a, c, e) non-catalytic (b, d, f) catalytic respectively.	208
Fig. 7.12	Bio-oil component distribution from non-catalytic and catalytic pyrolysis (a) classification based on carbon number (b) chemical composition and energy yield of bio-oil.	209
Fig. 7.13	The main oxygen components distribution in bio-oil from (a) non-catalytic (b) catalytic pyrolysis of coal (CL), microalgae (ALG) and coal-microalgae blend (CLALG) with synthesized Cu-Cr-ZSM-5 catalyst at a ratio of 1:1.	210
Fig. 7.14	The main nitrogen components distribution in bio-oil from (a) non-catalytic and (b) catalytic pyrolysis of coal (CL), microalgae (ALG) and coal-microalgae blend (CLALG) with synthesized Cu-Cr-ZSM-5 catalyst at a ratio of 1:1.	211
Fig. 7.15	Proposed reaction pathway of noncatalytic and catalytic pyrolysis of coal and de-oiled microalgae blend (CLALG) with synthesized Cu-Cr-ZSM-5 catalyst.	217

LIST OF TABLES

Table 2.1	Physicochemical characteristics and heavy metal concentration of water discharged from some representative coal mines in different countries.	17
Table 2.2	Summary of bioremediation and growth performance of microalgae cultures cultivated in different saline wastewater sources.	25
Table 2.3	Summary of heavy metal bioremediation from wastewater using microalgae.	26
Table 2.4	Detail process conditions and fatty acid methyl ester production through transesterification of microalgae biomass for bio-oil conversion.	34
Table 3.1	Mathematical expressions of $f(x)$ and $g(x)$ for the most applied solid-state kinetic models.	59
Table 3.2	Physico-chemical characteristics of coal mine effluent and nutrient supplemented coal mine effluent.	64
Table 3.3	Basic fuel characteristics for freshwater and marine microalgae species.	67
Table 3.4	Biomass characterization of fresh and marine microalgal cultures, cultivated in nutrient supplemented coal mine effluent.	69
Table 3.5	One-way ANOVA for microalgae fuel characteristic variables.	70
Table 3.6	Spearman's rank correlation estimation for different microalgae fuel characteristics.	71
Table 3.7	Kinetic parameter calculation of microalgae at main pyrolysis stage (230 – 370 °C) using different reaction models of Coats Redfern method.	79
Table 3.8	Comparison of activation energy calculated by present study with reported in the literature.	84
Table 3.9	Thermodynamic properties of different microalgae sp. at main pyrolysis stage (230-370 °C) by applying Coats Redfern and DAEM method.	85
Table 3.10	Summary of thermodynamic properties of different biomass materials.	86
Table 3.11	The performance comparison of different deep neural network structure.	89
Table 4.1	Average nutrient removal performance of all cycles (1–5) under semi-batch operation with different medium replacement ratios.	105
Table 4.2	Summary of the fatty acid methyl ester profile of <i>C. pyrenoidosa</i> sp. harvested after end cycle of HRT 6 d through semi-continuous cultivation in NSCME.	106
Table 4.3	Comparative assessment of ICP-MS results of NSCME desalination.	111
Table 5.1	Particle size distribution of the investigated low-rank coal sample.	119
Table 5.2	Factors and levels of microalgae-blended coal composites (MBCCs) production.	122
Table 5.3	Basic fuel characteristics of investigated waste coal, microalgae and microalgae blended coal composites (MBCCs).	125

Table 5.4	Box- Behnken design matrix and results for microalgae blended coal composites (MBCCs) production.	126
Table 5.5	Uncertainty estimation of each parameter by Monte Carlo simulation.	128
Table 5.6	Quadratic polynomial equations for the compressive and drop strength of microalgae blended coal composites (MBCCs) production.	129
Table 5.7	Model coefficient estimate by multiple regression analysis for compressive strength and drop strength of microalgae blended coal composites (MBCCs) production.	129
Table 5.8	Analysis of variance for different responses (compressive strength and drop strength).	130
Table 5.9	Comparison of mechanical performance of prepared composites in initial, individual and multi-objective optimized conditions.	137
Table 5.10	Summary of FTIR characterization of low-rank coal, de-oiled microalgae biomass, and MBCCs (MBCC1, MBCC2, and MBCC3).	139
Table 5.11	Combustion characteristics of the low-rank coal, de-oiled microalgae biomass and MBCCs at different optimization conditions.	143
Table 5.12	Comparative performance assessment of different coal-biomass densification studies.	144
Table 6.1	Experimental parameters and their levels to optimize hymethane carrying ratio via central composite design.	158
Table 6.2	Fuel characteristic analysis of coal and de-oiled microalgae blends.	162
Table 6.3	Estimation of characteristic temperatures for de-oiled microalgae and coal co- pyrolysis.	163
Table 6.4	Activation energy determination of de-oiled microalgae and coal blended material by using isoconversional KAS and STK method.	167
Table 6.5	A two-level full-factorial central composite design matrix in real value and coded unit (in parenthesis) with different responses for syngas production during co-pyrolysis of de-oiled microalgae, coal and blends.	172
Table 6.6	Model coefficient estimation by multiple regression analysis for enhancing hymethane carrying ratio at different pyrolysis characteristic temperatures.	173
Table 6.7	Quadratic polynomial equations for enhancing hymethane carrying ratio at different pyrolysis characteristic temperatures.	173
Table 6.8	Analysis of variance for enhancing hymethane carrying ratio at different pyrolysis characteristic temperatures.	174
Table 6.9	Comparison of hymethane carrying ratio from co-pyrolysis of coal-microalgae blends at different optimization conditions.	178
Table 7.1	Fuel characteristic analysis of coal (CL), de-oiled microalgae (ALG) and blend of coal and de-oiled microalgae (CLALG).	189
Table 7.2	XRD findings of synthesized Cu-Cr loaded ZSM-5 catalyst.	195
Table 7.3	Main chemical components present in bio-oil derived from catalytic and non-catalytic pyrolysis of coal and de-oiled microalgae blends.	211

Table 7.4	Physicochemical comparison of bio-oil from catalytic and non-catalytic pyrolysis of coal and de-oiled microalgae blend with ASTM grade oil and mineral oils.	214
Table 7.5	Summary of recently performed studies to upgrade pyrolysis bio-oil quality by applying different metal-loaded zeolite catalysts.	214

ABBREVIATIONS

ALG	De-oiled microalgae
AMD	Acid mine drainage
ANN	Artificial neural network
ANOVA	Analysis of variance
APHA	American Public Health Association
ASTM	American society for testing materials
BCR	Bubble column reactor
BET	Brunauer-Emmett-Teller
CCD	Central composite design
CL	Low rank coal
CLALG	Coal and de-oiled microalgae blend
CME	Coal mine effluent
CN	Cetane number
COD	Chemical oxygen demand
Conv1D	One-dimensional convolutional neural network
CR	Coats Redfern
DAEM	Distributed activation energy model
DCW	Dry cell weight
DTA	Differential thermal analysis
DTG	Derivative thermogravimetric
DNN	Deep neural network
EC	Electric conductivity
EDS	Energy dispersive X-ray spectroscopy
EPA	Environmental protection agency
FAME	Fatty acid methyl esters
FAO	Food and agriculture organization
FFBP	Feed-forward backpropagation
FTIR	Fourier transform infrared spectroscopy
GCV	Gross calorific value
GC-MS	Gas chromatography-mass spectrometry
GHGs	Greenhouse gas emission
HHV	High heating value
HRT	Hydraulic retention time
ICP-MS	Inductively coupled plasma mass spectrometry
IV	Iodine value
KAS	Kissinger- Akahira-Sunose
LHV	Low heating value
LM	Levenberg-Marquardt
LSTM	Long short-term memory
MBCCs	Microalgae-blended coal composites
MAE	Mean absolute error
MSE	Mean square error
MOGA	Multi-objective genetic algorithm
MUFA	Monounsaturated fatty acid
NSCME	Nutrient supplemented coal mine effluent
ORP	Open raceway pond
PAH	Polyaromatic hydrocarbon
PHA	polyhydroxyalkanoates

PReLU	Parametric rectified linear unit
PUFA	Polyunsaturated fatty acids
RSM	Response surface methodology
RMSE	Root mean square error
SDGs	Sustainable development goals
SEM	Scanning electron microscopy
SFA	Saturated fatty acids
STK	Starink
SV	Saponification value
TGA	Thermogravimetric analysis
TEM	Transmission electron microscopy
TDS	Total dissolved solid
TOC	Total organic carbon
WRI	Water resistance index
XRD	X-ray diffraction

NOTATIONS

A	Pre-exponential factor
α	Conversion degree
β	Heating rate
cSt	Centistokes
E_a	Activation energy
pH	Potential of hydrogen
h	Planck's constant
k	Boltzmann constant
ΔH	Enthalpy change
ΔG	Gibbs free energy change
ΔS	Entropy change
k	Rate constant
MPa	Mega pascal
R	Universal gas constant
R^2	Regression coefficient
rpm	Revolution per minute
T	Absolute temperature
t_d	Doubling time
T_i	Ignition temperature
T_p	Peak temperature
T_b	Burnout temperature
T_{p1}, T_{p2} and T_{p3}	Temperature of first, second and third peak in DTG curve
r_s	Spearman's rank correlation coefficient
μ	Specific growth rate
k	Rate constant
v/v	Volume by volume
g/g	Gram per gram
m^2/g	Square meter per gram
kJ/mol	Kilojoule per mole
J/s	Joule per second
J/K	Joule per kelvin
J/mol•K	Joule per mole per kelvin
MJ/Kg	Megajoule per kilogram
MJ/m ³	Megajoule per cubic meter
kg/m ³	Kilogram per cubic meter
$\mu V/s/mg$	Microvolts per milligram
%/ °C	Percent per degree celsius
°C/min	Degree Celsius per minute
$\mu mol\ photon/m^2/s$	Micromole photons per meter square per second
wt.%/ °C	Weight percent per degree celsius
mmol/g	Millimol per gram
mL/min	Milliliter per minute
$g\ L^{-1}$	Gram per liter
d^{-1}	Per day
cm^{-1}	Per centimeter
$mg\ L^{-1}\ d^{-1}$	Milligram per liter per day
$kg\ m^{-2}\ d^{-1}$	Kilogram per square meter per day
$kg\ d^{-1}$	Kilogram per day

mS cm ⁻¹	Millisiemens per centimeter
t yr ⁻¹	Ton per year
min	Minute
s	Second
h	Hour
ha	Hectare
L	Liter
ml	Milliliter
cm	Centimeter
μm	Micrometer
nm	Nanometer
%	Percent
°C	Degree Celsius
K	Kelvin
kV	Kilo volt
μL	Microliter
yr	Year
